# Environmental fluctuations lead to predictability in Sin Nombre hantavirus outbreaks

Angela D. Luis, 1,2,3,6 Richard J. Douglass, 4 James N. Mills, 5 and Ottar N. Bjørnstad 1,3

<sup>1</sup>Department of Entomology, Pennsylvania State University, University Park, Pennsylvania 16802 USA
<sup>2</sup>Department of Ecosystem and Conservation Sciences, University of Montana, Missoula, Montana 59812 USA
<sup>3</sup>Fogarty International Center, National Institutes of Health, Bethesda, Maryland 20892 USA
<sup>4</sup>Department of Biology, Montana Tech of the University of Montana, Butte, Montana 59701 USA
<sup>5</sup>Population Biology, Ecology, and Evolution Program, Emory University, Atlanta, Georgia 30322 USA

Abstract. Predicting outbreaks of zoonotic infections in reservoir hosts that live in highly fluctuating environments, such as Sin Nombre virus (SNV) in deer mice, is particularly challenging because host populations vary widely in response to environmental conditions and the relationship between field infection rates and abundance often appears to contradict conventional theory. Using a stage-structured host-pathogen model parameterized and cross-validated from a unique 15-year data set, we show how stochastic population fluctuations can lead to predictable dynamics of SNV in deer mice. Significant variation in host abundance and the basic reproductive number of the virus results in intermittent crossing of the critical host population density necessary for SNV endemicity and frequent local extinctions. When environmental conditions favor growth of the host population above the threshold, host-pathogen interactions lead to delayed density dependence in reservoir prevalence. The resultant ecological delay may provide a neglected opportunity for outbreak prediction in zoonoses.

Key words: critical host density; deer mice; delayed density dependence; ecological cascade; ecological forecasting; Peromyscus maniculatus; Sin Nombre virus; zoonoses.

#### Introduction

Many of the animal reservoir hosts of important human pathogens live in highly variable environments that induce strong ecological cascade effects in their dynamics (Jones et al. 1998, Saitoh and Takahashi 1998, Linthicum et al. 1999, Ostfeld and Keesing 2000, Kausrud et al. 2007). Predicting outbreaks of these infections is particularly challenging because reservoir abundance can consequently be extremely variable in space and time. Sin Nombre virus (SNV) circulates in wild deer mice (Peromyscus maniculatus; see Plate 1), causes hantavirus pulmonary syndrome (HPS) with 30–40% case fatality in humans, and is a classic illustration of the complexity of the interaction among climate, animal host ecology, and zoonoses (Parmenter et al. 1993, Yates et al. 2002). SNV was first recognized in 1993 after it caused an outbreak of HPS in the southwestern United States (CDC 1993). Human-to-human transmission is extremely rare, and this deadly outbreak was linked to increased primary productivity, high mouse density, and zoonotic transmission after an El Niño event brought increased precipitation to this usually arid region (Parmenter et al. 1993, Yates et al. 2002). This highlights the importance of understanding the reservoir host and pathogen dynamics, which can be key in controlling and preventing HPS and other zoonoses. However, when SNV is present in a local mouse population, it does not seem to follow typical temporal patterns of incidence or prevalence expected for a directly transmitted pathogen. For example, one would expect to see increased prevalence with increased density. However, the field data are mixed, only rarely showing a positive correlation between mouse density and SNV infection prevalence in the mouse population (Boone et al. 1998), and often showing either no relationship (Mills et al. 1997, Calisher et al. 1999) or inverse density dependence with higher prevalences at lower densities (see Appendix: Fig. A1; Douglass et al. 2001, Calisher et al. 2005).

We apply a quantitative approach in a highly variable zoonotic system to understand when there is increased risk of HPS and also to examine how the key theoretical concepts in disease ecology, such as the basic reproductive number ( $R_0$ , the expected number of secondary cases from a single case in a fully susceptible population) and the critical host density (Nc) in governing invasion of pathogens with density-dependent transmission, relate to highly variable systems. We formulate a stage-structured (age class) SI (susceptible-infected) model for the deer mouse-SNV interaction, which we parameterize from 15 years of monthly field data from a site in Cascade County, Montana, USA, (Fig. 1) and validate against data from a separate field site near Polson, Montana, USA, with very different temporal patterns of host abundance and virus prevalence. We analyze how stochastic (e.g., climatic) forcing of demographic rates affects the pathogen

Manuscript received 9 October 2014; accepted 5 November 2014. Corresponding Editor: S. J. Schreiber.

<sup>6</sup> Present address: Department of Ecosystem and Conservation Sciences, University of Montana, Missoula, Montana 59812 USA. E-mail: Angela.Luis@umontana.edu

dynamics, how the pathogen affects the host population dynamics, and the conditions required for circulation of the virus.

## **M**ETHODS

#### The model

Our epidemiological model includes background host population dynamics with three functional age classes, juveniles (J), subadults (SA), and adults (A), and since infection is life-long (Mills et al. 1999a), two classes with respect to the virus, susceptible (S) or infected (I), determined by antibody positivity. To reduce the dimensionality of the model, we omit a juvenile-infected class, because juvenile infection in nature is very rare and antibodies when they do occur are likely maternally derived. Similarly, host sex is not included, although sex differences may be important at the individual scale (e.g., Kuenzi et al. 2001, Douglass et al. 2007); males and females are considered the same. This leads to five host classes: juveniles (J), susceptible subadults  $(S_{SA})$ , infected subadults  $(I_{SA})$ , susceptible adults  $(S_A)$ , and infected adults  $(I_A)$ . The model includes logistic growth (after Gao and Hethcote 1992), where the host population experiences density dependence in both birth and death rates, which are determined by a time-varying carrying capacity,  $K_t$ . Transmission is assumed to be density dependent (Luis et al. 2012), and maturation from juveniles to subadults is assumed constant  $(m_1)$ . Because the presence of adults is known to inhibit subadults from maturing and becoming reproductive (Millar 1989), we assume maturation from subadult to adult depends on the density of adults, where  $m_2$  is the maximum maturation rate (in the absence of adults). We include a parameter for disease-induced mortality (µ), since we recently documented that SNV infection decreases deer mouse survival (Douglass et al. 2001, 2007, Luis et al. 2012). The resulting set of equations is

$$\frac{dJ}{dt} = A\left(b - ar\frac{N}{K_t}\right) - J\left(d + (1 - a)r\frac{N}{K_t}\right) - Jm_1$$

$$\frac{dS_{SA}}{dt} = Jm_1 - S_{SA}\left(d + (1 - a)r\frac{N}{K_t}\right) - \beta_1 S_{SA}I$$

$$- S_{SA}m_2\left(1 - \frac{A}{K_t}\right)$$

$$\frac{dI_{SA}}{dt} = \beta_1 S_{SA}I - I_{SA}\left(\mu + d + (1 - a)r\frac{N}{K_t}\right)$$

$$- I_{SA}m_2\left(1 - \frac{A}{K_t}\right)$$

$$- I_{SA}m_2\left(1 - \frac{A}{K_t}\right)$$

$$\frac{dS_A}{dt} = S_{SA}m_2\left(1 - \frac{A}{K_t}\right) - S_A\left(d + (1 - a)r\frac{N}{K_t}\right) - \beta_2 S_AI$$

$$\frac{dI_A}{dt} = \beta_2 S_AI + I_{SA}m_2\left(1 - \frac{A}{K_t}\right)$$

$$- I_A\left(\mu + d + (1 - a)r\frac{N}{K_t}\right)$$
(1)

where N is the total population size, A is the adult population size  $(S_A + I_A)$ , I is the total number of infected individuals for both age classes  $(I_{SA} + I_A)$ , b is the maximum birth rate (in absence of density dependence, i.e., when N = 0), d is the minimum death rate, and a is the proportion of density dependence due to density dependence in birth rates. If a = 0, then birth rates are density independent, and all the density dependence seen is due to density dependence in the death rates, and conversely, if a = 1, then all the density dependence is in the birth rates. r is b - d.  $\beta_1$  is the transmission rate for subadults, and  $\beta_2$  is the transmission rate for adults. As a secondary analysis, we estimated the importance of immigration of infected mice. For this, we added a constant immigration term,  $\phi$ , to  $dI_A/dt$ . The transmission rates estimated without immigration may then be too high to fit the observed dynamics, so at the same time, we estimated an additional parameter,  $\alpha$ , as a multiplier on the transmission rates. For instance,  $\beta_2 S_A I$  is replaced with  $\alpha \beta_2 S_A I$ . All of the parameters were estimated using field data. Tables 1 and 2 summarize all variables and parameters with respective maximum likelihood esti-

For our model the basic reproductive number for a population at equilibrium is

$$R_0 = \frac{\beta_1 N^* D_{SA} + \beta_2 N^* D_A}{\mu + d + (1 - a)rp}$$
 (2)

19399/170, 2015, 6, Downloaded from https://esajournals.on/helibaray.wiley.com/doi/10.1890/14-1910.1 by Cochanne Uruguay, Wiley Online Library on [20/10.0225]. See the Terms and Conditions (https://onlinelibrary.wiley.com/terms-and-conditions) on Wiley Online Library of rules of use; OA articles are governed by the applicable Creative Commons License

where  $N^*$  is the equilibrium population size, and D is the stable age distribution, so that  $D_{SA}$  and  $D_A$  are the proportion of the population that is made up of subadults and adults, respectively, at equilibrium. For a population not at equilibrium due to fluctuations in the carrying capacity,  $N^*D_{SA}$  and  $N^*D_A$  could be replaced with  $SA_t$  and  $A_t$ , and p could be replaced with  $N_t/K_t$ . However, this will still be an approximation for time-varying systems because the vital rates and age distribution may change over time (see *Discussion*).

Since the virus has density-dependent transmission, and  $R_0$  is a function of density, there will be a critical host density,  $N_c$ , below which the virus cannot invade (when  $R_0$  falls below 1; Anderson 1981). For our model, the critical host density is

$$N_c = \frac{\mu + d + (1 - a)rp}{\beta_1 D_{SA} + \beta_2 D_A}.$$
 (3)

In the absence of disease, the population reaches the disease-free equilibrium,  $N_{\rm DF}^* = pK$ , where p is a constant of proportionality. Note that this equilibrium is less than K (by about 12% with the given vital rates) because of the age-structured interactions and the presence of nonreproducing age classes. K would be the population size if juveniles contributed to reproduction. Increasing K leads to a linear increase in  $R_0$  and a nonlinear increase in the equilibrium prevalence once the critical host density,  $N_c$ , is exceeded (Appendix: Fig. A3).

1693

19399/10, 2015, 6, Downloaded from https://esajournals.on/heibtrary.wikey.com/doi/10.1890/14-1910.1 by Cochanne Uruguay, Wiley Online Library on [20/10.025]. See the Terms and Conditions (https://onlinebbrary.wiley.com/rems-and-conditions) on Wiley Online Library or rules of use; OA articles are governed by the applicable Creative Commons License

Fig. 1. Deer mouse density (solid black line) over the study period in relation to the critical host density,  $N_c$  (dotted black line), as well as density of infected mice (red line; scale on right) at the Cascade field site (Cascade County, Montana, USA).

#### Data

To parameterize the model, we used 15 years of monthly mark-recapture data from two trapping grids (3 km apart) in Cascade County, central Montana, USA (46°59.3' N, 111°35.3' W) from June 1994 through December 2008. This site is an agricultural grassland supporting an active, low-density cattle ranch. To validate the model, we used out of sample data from a trapping grid near Polson, Montana, USA (47°38.4′ N, 114°20.7′ W). This site, 220 km from the Cascade site, is sagebrush scrub occasionally grazed by cattle. Deer mice accounted for over 85% of the small mammal assemblage (Douglass et al. 2001). Live-trapping occurred for three consecutive nights each month at the Cascade grids. The Polson grid was not trapped during the winter months. Grids consisted of 100 trap stations equally spaced in a square of 1 ha with one Sherman live trap (H. B. Sherman Traps, Talahassee, Florida, USA) per station. Individuals were tagged with uniquely numbered ear tags and classified into age classes based on weight according to the definitions of Fairbairn (1977). Since the mouse abundances on the two grids at Cascade were significantly correlated (Pearsons product moment correlation test on minimum number alive (MNA); R =0.77, P < 0.001; Luis et al. 2010), data from the two grids were lumped together. Since infection is lifelong, individuals were considered infected if they had detectable antibodies to SNV (except for juveniles, as explained in Methods) by enzyme-linked immunosorbent assay (Mills et al. 1999a) at the Montana Department of Health and Human Services or at Viral Special Pathogens Branch, Centers for Disease Control and Prevention, Atlanta, Georgia, USA. For a detailed description of the field and laboratory methods, see Douglass et al. (2001).

## Parameter estimation

We used mouse captures on the two grids as an index for density of the five classes. The disease-induced reduction in monthly survival probability for infected deer mice was estimated using mark–recapture statistical modeling (Luis et al. 2012). This probability was converted to a rate for the estimate of disease-induced mortality,  $\mu$  (according to rate =  $-\log(1 - \text{probability})$ /

 $\Delta t$ , where  $\Delta t$  is the trapping interval). We numerically integrated the ODEs (Eq. 1) using the Isoda function from the deSolve package for R software (R Development Core Team 2010). Since we did not have an independent measurement of the time varying K, we estimated this function nonparametrically (using smoothing splines) using a two-step protocol. We first used the simplifying assumption that density reflected  $K_t$ with a few months time lag. The crude assumption in this first step is that demographic change is relatively fast compared to environmental change. We investigated various time lags, but finally used a smoothed spline of the MNA four months ahead as our initial proxy of  $K_t$ . Conditional on this, we estimated the remaining parameters in the model from the mouse time-series data using trajectory-matching (Wood 2001) maximum likelihood, assuming Poisson errors (e.g., Bolker 2008). For this, we numerically minimized the negative loglikelihood between the model and the vectors of abundance for the five classes over the whole trajectory (i.e., trajectory matching) using the Nelder-Mead algorithm implemented in the optim function. For the statistical estimation, we assume that all of the parameters are nonnegative, and a to be a proportion, constrained to the interval 0-1. Parameters were constrained using inverse log or logit transforms, as appropriate. In the second step, we used these estimated parameter values to produce a maximum likelihood estimate of the time-varying carrying capacity,  $K_t$ , by optimizing the coefficients (as done for the other parameters) of the basis functions of a polynomial

TABLE 1. Notation used to denote model variables.

Variables	Definition
J S <sub>SA</sub> I <sub>SA</sub> S <sub>A</sub> I <sub>A</sub> A I N K N* N* DF	number of juveniles number of susceptible subadults number of infected subadults number of susceptible adults number of infected adults total number of adults total number of infected individuals total number of individuals carrying capacity equilibrium population size disease-free equilibrium population size

TABLE 2. Model parameters, their maximum likelihood estimates (with CI in parentheses), and definitions.

Parameters	Maximum likelihood estimate	Definition
b	0.315 (0.295–0.337)	maximum birth rate (when $N = 0$ )
d	0.315 (0.295-0.337) $3.66 \times 10^{-5} (2.13 \times 10^{-12}-627)$	minimum death rate (when $N=0$ )
а	0.614 (0.607–0.622)	proportion of the density dependence attributable to births
$m_1$	2.12 (1.92–2.33)	maturation rate from juvenile to subadult
$m_2$	1.05 (0.941–1.17)	maximum maturation rate (when $A = 0$ ) from subadult to adult
$\beta_1$	$3.87 \times 10^{-3} (3.22 \times 10^{-3} - 4.66 \times 10^{-3})$	transmission rate for subadults
$\beta_2$	$1.50 \times 10^{-2} (1.46 \times 10^{-2} - 1.53 \times 10^{-2})$	transmission rate for adults
ф	0.033 (0.015–0.073)	constant immigration rate of infected adult mice
ά	0.770 (0.642–0.862)	multiplier on transmission rates for models with immigration
r	0.315	$b-\hat{d}$
p	0.879	proportion of $K$ that is the disease-free equilibrium $(N_{DF}^* = pK)$ found numerically
μ	0.085	disease-induced mortality rate (Luis et al. 2012)
$D_{\mathrm{SA}}$	0.215	proportion of the population made up of subadults at $N_{DE}^*$
$D_{\mathrm{A}}$	0.737	proportion of the population made up of adults at $N_{DF}^*$

Note: All rates are per month.

spline with 10 degrees of freedom (chosen to select the smallest degrees of freedom that showed the overall trend in the data). For simplification, these methods assume that all the error between the model and the data is measurement error and that all environmental process stochasticity is captured by the time-varying  $K_t$ .

#### Analysis

 $R_0$  and  $N_c$  were calculated by setting  $dI_{SA}/dt + dI_A/dt$ = 0 (Anderson 1991). To analyze the lags between population density and antibody prevalence, we used the cross-correlation function (CCF) to find the lag that gave the largest correlation for both the data and model. We also ran simulations using a push disturbance, from K = 25 to K = 60, to determine the effect of the different parameters on the dynamics. Elasticities of the parameters were calculated by individually increasing each parameter  $(b, d, m_1, m_2, \beta_1, \beta_2, a, \text{ and } \mu)$  by 5% and determining the percentage of change in the lag between maximum density and maximum prevalence. We also ran simulations with different values of K and determined the time lag between maximum density and maximum prevalence. Additionally, for different values of K, starting from equilibrium in the absence of infected individuals, we determined how long it took to reach five infected individuals from one initial infection. Although it is difficult to set a threshold level above which the public is at greater risk, five infected individuals per hectare is above the background level seen at the Cascade site.

There were multiple colinearities in the parameters (see Appendix: Fig. A6 for profile likelihoods), so the the variance–covariance matrix was not definite positive. Therefore, we used the Moore-Penrose generalized inverse of the Hessian (pseudoinverse in the corpcor package in R) and a generalized Cholesky decomposition (gchol in the bdsmatrix package) to produce a pseudo-variance matrix (Gill and King 2004). To get a measure of uncertainty for our estimate of  $N_c$ , using myrnorm in the MASS package of R (Venables and Ripley 2002), we took 1000 random samples from the

multivariate normal distribution, using our parameter estimates as the means, and the pseudo-variance—covariance matrix. Using these parameter values, we determined the interquartile range for  $N_{\rm c}$  (Bolker 2008).

## Model validation

19399170, 2015, 6, Downloaded from https://esajournals.onhelibtrary.wiley.com/doi/10.18901/4-1910.1 by Cochanne Uruguy, Wiley Online Library on [20/10.025]. See the Terms and Conditions (https://onlinebbrary.wiley.com/rems-and-conditions) on Wiley Online Library or rules of use; OA articles are governed by the applicable Creative Commons License

To validate the model, we used MNA and MNI (minimum number infected) estimates from the trapping grid near Polson, Montana, USA. The correlation of the times series of mouse abundances between the Cascade and Polson sites were low (R = 0.26). The demographic and epidemiological parameter estimates  $(b, d, m_1, m_2,$  $\beta_1$ ,  $\beta_2$ , a, and  $\mu$ ) for the Cascade site were used here. Since cross-correlation analysis revealed that MNA lagged behind  $K_t$  by approximately three months for the Cascade site, we set the time-varying  $K_t$  for the Polson model to a smoothed spline of the MNA at this site three months ahead. This site was not trapped over winter. To fill in the missing months, we interpolated mouse MNA linearly between the last fall measurement and the first spring measurement. All other parameters were set to those estimated from the Cascade site (independent from validation data). Pearson's product moment correlation test and Bartlett's test was used to compare the number of infected mice at Polson to the out of sample model predictions for the corresponding time points.

### RESULTS

Maximum likelihood estimates of the model parameters are given in Table 2. Using these parameter estimates, we estimate the critical host density to be 17 mice/ha (interquartile range 7–35). The mouse population was below this critical threshold 57% of the time at the Cascade field site (Fig. 1).  $R_0$  ranged from 0.19 (when the population was at its lowest density) to 5.73 (at highest density), with a mean of 1.27 and a median of 0.96.

We estimate the time-varying carrying capacity,  $K_t$ , nonparametrically using a smoothing spline (Fig. 2A,

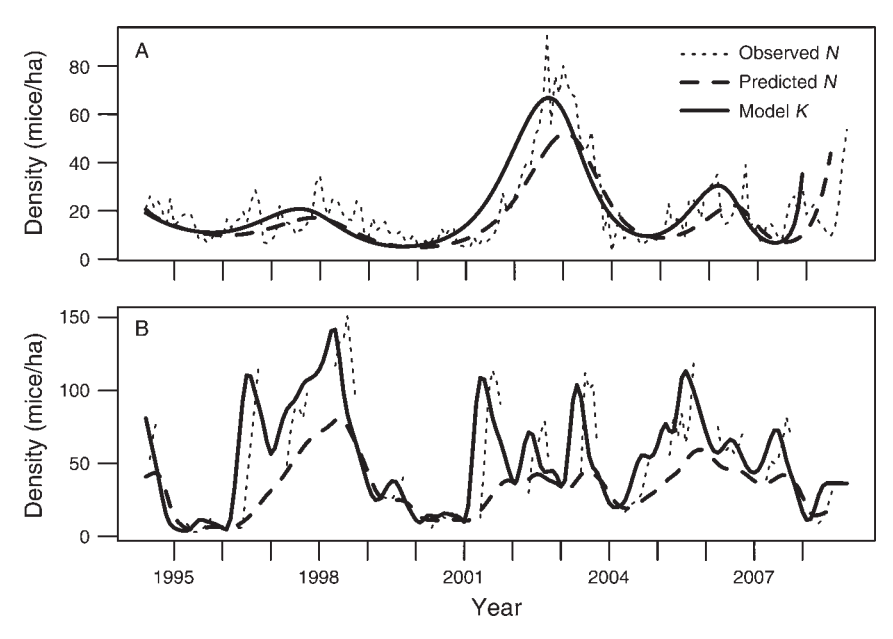


Fig. 2. Mouse population density observed (light dashed line), the carrying capacity, *K* (heavy solid line), and model simulated density (heavy dashed line) for the (A) Cascade and (B) Polson (Polson, Montana, USA) sites. *K* for the Cascade site was estimated as a smoothed spline with 10 degrees of freedom. For the Polson site, MNA (minimum number alive) three months ahead (with winter months interpolated) was used as a proxy for *K*. *N* is mice/ha.

heavy solid line). The cross-correlation function (CCF) reveals that the rodent abundance generally lags behind  $K_t$  by three months (CCF(3) = 0.856), which is not surprising given our original assumption used for demographic parameter estimation. However, this lag is slightly longer when the population is increasing and less when the population is decreasing (Fig. 2A).

Our previous work has shown that SNV-induced mortality ( $\mu$ ) can be significant in the natural rodent host (Douglass et al. 2001, 2007, Luis et al. 2012). Disease-induced mortality was estimated from a mark-recapture study as described in Luis et al. (2012), and as we discussed there, this is likely to be an underestimate, due to the combination of incubation period, time to detectable antibodies, and intertrapping interval. Therefore, we explored the effect of varying  $\mu$  on the pathogen dynamics. The disease-induced mortality affects both  $R_0$  and the critical host density. With the estimated parameters, if there was no disease-induced mortality, the critical host density would be as low as 9 mice/ha; increasing  $\mu$  from 0.085 to 0.2 would increase the critical host density to 26 mice/ha.

The presence of disease-induced mortality also demonstrates that SNV has the potential to regulate its host below the disease-free equilibrium. The strength of the impact on the population is largely determined by the prevalence, which is a function of previous density and the carrying capacity (Appendix: Fig. A3). During the study, SNV infection prevalence reached as high as 30%, during which time our model suggests the host population had been regulated to almost 20% below the disease-free equilibrium.

Although we have assumed density-dependent transmission, the prevalence is not predicted to increase with density in an instantaneous fashion. On the contrary, the model predicts environmental fluctuations to induce an overall negative relationship between current density and prevalence at the Cascade site and an overall pattern of delayed density-dependence in prevalence. Both of these predictions are clearly borne out in the data (Appendix: Figs. A1, A2). These patterns are due to fluctuations in the mouse population. The dominant lag between a peak in abundance and a peak in prevalence for the Cascade site was 16 months in the data (R = 0.367, P < 0.0001, CCF = 0.348; Appendix: Fig. A2a), exactly as predicted by the model (R = 0.90, P < 0.0001, CCF = 0.737; Appendix: Fig. A2b). This 16-month lag is a result of the dominant peak in mouse abundance and the subsequent peak in mouse infection prevalence (Fig. 1).

The simulated mouse abundance and infected mouse abundance from the model without immigration are a little behind those in the data (Fig. 3A), potentially due to the smoothing of K and the deterministic model framework lacking immigration of infected mice, as discussed in *Discussion*. Therefore, we added an immigration rate to the infected adult class. A constant monthly immigration of 0.033 infected mice per month and a corresponding 23% reduction in the transmission rate improved the fit to the major outbreak that occurred in the Cascade data (Fig. 3B). These changes to the model raise the estimate of the critical host density slightly to 18 mice/ha.

Using simulations, we find that the lag between a peak in density and a peak in prevalence when the population

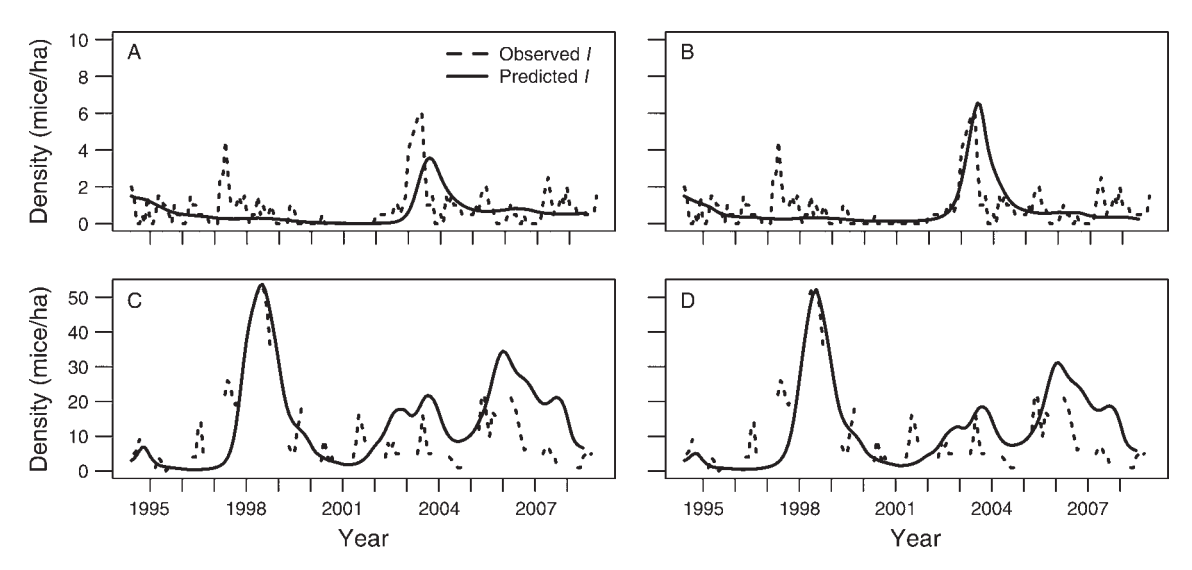


Fig. 3. Density of infected mice observed (thin dashed line), and model predicted (black solid line) for the (A and B) Cascade and (C and D) Polson field sites. Panels (A and C) show model fit without an immigration term and panels (B and D) show model fit with an immigration term. *I* is the total number of infected individuals for both age classes.

is allowed to come to equilibrium is inversely related to  $R_0$  (Fig. 4B, dashed line). With higher K values, the population reaches equilibrium and maximum prevalence faster (Fig. 4A) because of the associated increase in  $R_0$ . To illustrate, for various constant K values, starting from equilibrium in the absence of infected individuals, we analyze how long it will take to reach five infected individuals from one initial infection (above background levels; Fig. 4B). The predicted time lag ranged from 37 to 4 months, as K was varied from 25 to 75. This illustrates how the 16-month lag that was dominant at the Cascade site was a result of how high the population density reached and for how long during 2002 and 2003 (Fig. 1). If there had been a larger peak in mouse density, the peak CCF would occur at a shorter lag. The elasticity analysis indicated that the transmission rate of the adults,  $\beta_2$ , is the most influential parameter on the lag time, causing a 5.5% decrease in lag time with a 5% increase in the parameter value (Appendix: Fig. A5). The proportion of density dependence acting on births vs. deaths (a) was the most important demographic parameter (Appendix: Fig. A5). The confidence intervals for the maximum likelihood estimate of d were quite large, but the elasticity analysis reveals this parameter has little effect on the dynamics.

Although the temporal patterns of infected hosts differ significantly between the Cascade site and a distant site (independent data from parameter estimation, Polson, Montana; Pearson production moment correlation, P = 0.41, R = 0.09), our model parameterized from the Cascade site does a fair job at predicting the viral dynamics at this distant site (Fig. 3). The only input for the model was the initial values for the stage classes, and the proxy for the time-carrying capacity, MNA three months ahead. Model-predicted and observed-number infected have a correlation of R = 0.75

(correlation coefficient, with P < 0.01 by Bartlett's test) in this out of sample model validation. The addition of an immigration term to the model had little effect on the fit to the Polson data (Fig. 3C, D).

## DISCUSSION

19399/10, 2015, 6, Downloaded from https://esajournals.on/heibtrary.wikey.com/doi/10.1890/14-1910.1 by Cochanne Uruguay, Wiley Online Library on [20/10.025]. See the Terms and Conditions (https://onlinebbrary.wiley.com/rems-and-conditions) on Wiley Online Library or rules of use; OA articles are governed by the applicable Creative Commons License

This is the most comprehensive study to date of SNV and deer mouse population dynamics, including agestructured demographic and epidemiological parameter estimates, transmission rates,  $R_0$ , critical host density, and impact on the host population dynamics, using detailed, long-term demographic data. The analyses reveal that approximately 17 mice/ha are necessary for pathogen invasion, and 57% and 20% of the time at the Cascade and Polson sites, respectively, the population was below this critical threshold. This finding explains the sporadic disappearance of the virus and why most reintroductions of the virus result in stuttering chains of transmission rather than major epizootics. SNV in deer mice, therefore, appears to often be at the edge of local persistence: the virus persists at the metapopulation rather than local scale (Grenfell and Harwood 1997, Glass et al. 2000).

A critical consequence of host population fluctuations and frequent local extinction of the virus is the dominance of nonequilibrium and transient dynamics. The two most commonly used formulations for disease transmission are density-dependent and frequency-dependent transmission (McCallum et al. 2001). Under equilibrium conditions, density-dependent transmission results in a positive correlation between abundance and prevalence. Conversely, if transmission is frequency dependent, prevalence should remain roughly the same with varying host densities. Seemingly paradoxically, in SNV, we, as well as others (Douglass et al. 2001, Calisher et al. 2005), see a significantly negative

1697

While in the model transmission is in fact density dependent, it can take many months to reach equilibrium or a maximum in prevalence after an increase in the carrying capacity and a subsequent increase in mouse density, and often, before enough transmission occurs to generate an outbreak, the population density has begun to decline due to temporal decreases in the carrying capacity. Such nonequilibrium dynamics reduce the likelihood of outbreaks, because it is not enough for the mouse population to be above  $N_c$ , but it must be high enough for long enough to sustain a chain of transmission to produce an outbreak. In the southwestern United States, at least two years of high-risk conditions were necessary for SNV to reach high prevalence (Glass et al. 2002). Whenever the population density remains high enough for long enough, the lag between peak density and prevalence depends on all the demographic and epidemiological parameters (because they affect  $R_0$ ), as well as the timevarying carrying capacity. This explains why the delay in density dependence varies within and between field sites (Carver et al. 2011) in response to how the underlying carrying capacity differs between sites and at different times. As  $R_0$  or  $K_t$  increases, so does the rate of spread of the pathogen, allowing the system to approach equilibrium faster and thus decrease the time lag between peak density and prevalence (Fig. 4). In the same way that diseases with a lower  $R_0$  have a higher age at first infection (Anderson and May 1991), a more slowly circulating virus may take a number of months to build to a maximum prevalence after an increase in density. This delay allows for a potential opportunity to forecast increases in SNV infection in the mouse reservoir.

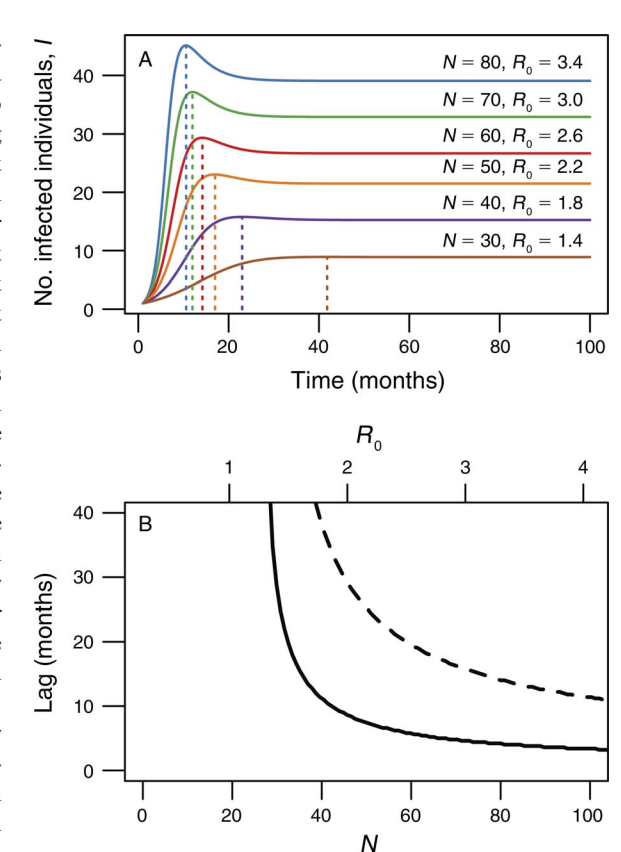


Fig. 4. (A) The number, N, of infected mice predicted over time at different population densities if we allow the population to come to an equilibrium. The dashed lines show when the infection peaks. As density is increased, the peak in I, the total number of infected individuals for both age classes (subadults and adults;  $I_{\rm SA} + I_{\rm A}$ ), is higher and occurs sooner. (B) The lag between a peak in density and the peak in prevalence (dashed line) when the population is allowed to come to equilibrium are negatively correlated with N (mice/ha) and  $R_0$  (the expected number of secondary cases from a single case in a fully susceptible population). The number of months it takes to reach five infected individuals from one initial infection (above background levels; solid line). For models with infected immigrants, the curves shift slightly to the right because of corresponding decreases in the transmission rate.

The model parameterized from the Cascade site was able to simulate the dynamics at the Polson site with  $R\!=\!0.75$ . Admittedly, the model is not able to replicate the somewhat stronger seasonality seen at the second site. Seasonality in birth rates and transmission (not included in the model) may explain why prevalence often peaks in the spring in more seasonal environments (Douglass et al. 2001, Kuenzi et al. 2005, Madhav et al. 2007). Note that the only input to the model for Polson was the local mouse abundance data three months ahead used as a proxy for the time-varying carrying capacity. Estimating the spline function for the carrying capacity, as we did at the Cascade site, was not done here, but could potentially improve the fit.

We find that immigration of infected individuals is important at Cascade, where the density is often below



PLATE 1. Juvenile deer mouse (Peromyscus maniculatus). Photo credit: A. D. Luis.

the critical host density and there is local fade-out of infection. There was more than a year in which there were no infected mice at the Cascade site, and the chain of transmission was broken. In our deterministic model, the number of infected mice dropped to a small fraction. When the carrying capacity eventually increased above the critical host density, the infection took longer to build from this low level than if there had been one infected mouse introduced. The addition of a constant immigration improved the fit to the major outbreak that occurred there. However, at Polson, where the density is consistently above  $N_c$  (and the chain of transmission is rarely broken), the addition of infected immigrants did not alter the dynamics substantially (Fig. 3). Even with the addition of immigration, we do not capture a smaller peak that occurred at Cascade in 1997. Perhaps surrounding areas were experiencing higher population densities and higher prevalences and leading to higher immigration of infected individuals.

The inherent lags between mouse density and infection prevalence may lead to the potential to forecast outbreaks. Once the mouse population density reaches above the critical host density of 17 mice/ha, there is a possibility of an outbreak if mouse density remains high. For example, if mouse population density reaches 40 mice/ha and remains there for six to eight months, an outbreak is likely. We call 5–10 infected mice/ha an

outbreak (above background levels seen at Cascade). Fig. 4 shows the time to reach five infected mice with the introduction of one infected mouse and also the time to reach equilibrium, which is significantly longer. Once the mouse population reaches this density, public officials could begin prevention strategies such as public announcements. If, instead, the mouse population increases from below  $N_c$  to only 25 mice/ha, there is a chance of an outbreak only if the density remains at that level for more than 18 months. So in this instance, there may be many months warning and more time for intervention strategies. For sites such as Cascade, which are at the edge of local persistence, it is likely that during those next 18 months the mouse population density will drop below  $N_c$  once again and an outbreak may never occur. Nevertheless, an understanding of the relationship between time lags in mouse density and infection prevalence provides additional warning for the potential for an outbreak.

Our theoretical quantifications of  $R_0$  and  $N_c$  provide important new insights into the maintenance and metapopulation dynamics of Sin Nombre hantavirus within the reservoir in Montana. We gain these insights using the broad-brush equilibrium assumptions that the rodent carrying capacity is constant and that stage structure is stationary. Obviously, these heuristic equilibrium assumptions are at odds with our overall take-

1699

home message that ecological transience, which was ever-present during the course of our study, is the source of intermediate-term predictability in hantavirus dynamics. For example, whenever the age structure of the fluctuating host population is skewed toward older individuals (which have a higher transmission rate),  $R_0$ would transiently be higher and  $N_c$  would be lower. Moreover, rodent vital rates depend on abundance  $(N_t)$ in relation to current carrying capacity  $(K_t)$ . When abundance is lower than K, infected (and all) mice tend to live longer, increasing their infectious period and opportunities to transmit the infection to others. In the real world, the infectious period will change over time in response to how abundance changes with respect to changes in  $K_t$ . We calculate that over the course of our study, the infectious period was variable with a mean of six months and an interquartile range of 4.6-6.9 months. Using a moving average over this range, we calculate an interquartile range of 12.6–18.3 for  $N_c$ . At any point in time, to truly know if one infected individual will replace itself over its lifetime would require knowledge of the future, what its infectious period will be, and the continuous trajectory of the age structure of the population over that period. The fact that both  $R_0$  and  $N_c$  are nonstationary and widely timevarying may require a shift in how we forecast risk of human spillover in this system.

We found that the rate at which adult mice become infected is almost four times greater than that for subadults ( $\beta_2$  and  $\beta_1$ , respectively; Table 2). This is probably due to much of the transmission occurring through aggressive contacts, which are more common in reproductively active individuals (Glass et al. 1988, Mills et al. 1997). This is consistent with numerous field studies showing that older, heavier mice are more likely to be infected (i.e., Abbott et al. 1999, Mills et al. 1999b, Douglass et al. 2001). A second reason for the age bias is that since the virus is often circulating with a low  $R_0$ , the mean age of infection will be high even when contact patterns are random (Anderson and May 1991).

Since SNV causes disease induced mortality (Luis et al. 2012), it has the potential to regulate the host population. Here, the strength of regulation largely depends on the prevalence of the virus, which is determined by the carrying capacity. During the study, prevalence reached as high as 30%, and during that time, the population will have been regulated to almost 20% below the disease-free equilibrium, according to our analysis. Although, in this system, the bottom-up control by climatic drivers appears to be the main driver in this system (Luis et al. 2010) and responsible for approximately 95% of the fluctuation in abundance in our model, SNV may nevertheless be a significant regulating force at high densities.

Disease-induced mortality also has important consequences for the disease dynamics. Disease-induced mortality effectively reduces the infectious period and decreases  $R_0$ , making the virus less likely to persist

How transmission scales with host density in wildlife populations is an open issue. There is evidence for density-dependent transmission (Ramsey et al. 2002), frequency-dependent transmission (transmission scales with the proportion infected; McCallum et al. 2009), and functions in between density- and frequency-dependent transmission (Smith et al. 2009). We focus here on density-dependent transmission, because it was supported in our capture-mark-recapture study (Luis et al. 2012) and provided good out of sample validation. Alternative transmission functions were explored, including frequency-dependent transmission, and two different flexible forms that could include transmission functions between density and frequency dependence. While these alternative transmission functions fit the original time series adequately, the density-dependent model provided the better out of sample validation (Appendix: Fig. A7).

This relatively simple deterministic model neglects several factors that may be important in the dynamics. Demographic stochasticity could increase estimates of  $N_c$  and decrease  $R_0$ , most often when I < 10. Testing the importance of demographic stochasticity, process noise, stochastic immigration of infected individuals, stuttering chains of transmission, and adding seasonality in demographic processes are the next steps to improve the fit of the model and understand the underlying processes driving the observed dynamics. Additionally, refinements of the estimates of the time-varying carrying capacity for both field sites, including environmental covariates (e.g., Luis et al. 2010), may be valuable in improving predictive power of the model.

Since we have very limited data on viral shedding, we must use antibodies as a marker of infection and infectiousness. Generally infection is lifelong, though in a few cases, antibodies may wane, and the virus may be undetectable for periods with viral recrudescence (Mills et al. 1999a, Kuenzi et al. 2005). There is some evidence for increased infectiousness in the first few months after infection (Botten et al. 2002), which could affect the dynamics. However, our model ignores these points and predicts the dynamics quite well, possibly because most mice do not live for more than a few months after antibody conversion.

Various studies focused in the southwestern United States have attempted to find refugia of endemic SNV circulation using remote sensing (Glass et al. 2002, 2007). Since densities at the Polson site were often above the critical susceptible density ( $N_c$ ), this habitat type may represent such a refugium in Montana. However, even at this site the chain of transmission was frequently broken and abundance was below  $N_c$  more than 20% of the time. Further research is therefore needed to identify habitat characteristics associated with rodent densities

above  $N_{\rm c}$  and whether SNV persists as a core-satellite metapopulation, where the infection is endemic in certain favorable patches, or whether long-term local persistence does not occur and persistence is only at the regional metapopulation scale (Grenfell and Harwood 1997).

Although further studies are needed to refine estimates and on the applicability of this approach to other systems, our study demonstrates that monitoring of zoonotic reservoir populations may provide advance warning of the possibility of an outbreak, potentially providing public health officials time to implement prevention strategies.

#### ACKNOWLEDGMENTS

We thank Dave Cameron and Dana Ranch, Inc., and the Confederated Salish and Kootenai Tribes at Polson for unlimited access to their properties, as well as Kent Wagoner for database management and design of specialty software. Scott Carver, Kevin Hughes, Arlene Alvarado, Farrah Arneson, Karoun Bagamian, Jessica Bertoglio, Brent Lonner, Jonnae Lumsden, Bill Semmons, and Amy Skypala provided valuable assistance in the field. S. Zanto provided serologic testing at the Montana State Department of Public Health and Human Services Laboratory; P. Rollin and A. Comer arranged serologic testing at the Special Pathogens Branch Laboratory, U.S. Centers for Disease Control and Prevention. Financial support was provided by the U.S. NIH grant P20RR16455-05 from the INBRE BRIN program, the U.S. CDC through cooperative agreement US3/CCU813599, and the Research and Policy for Infectious Disease Dynamics (RAPIDD) program of the Science and Technology Directorate (Department of Homeland Security) and the Fogarty International Center (NIH).

## LITERATURE CITED

- Abbott, K. D., T. G. Ksiazek, and J. N. Mills. 1999. Long-term hantavirus persistence in rodent populations in central Arizona. Emerging Infectious Diseases 5:102–112.
- Adler, F. R., J. M. C. Pearce-Duvet, and M. D. Dearing. 2008. How host population dynamics translate into time-lagged prevalence: an investigation of Sin Nombre virus in deer mice. Bulletin of Mathematical Biology 70:236–252.
- Anderson, R. 1991. Discussion: the Kermack-McKendrick epidemic threshold theorem. Bulletin of Mathematical Biology 53:1–32.
- Anderson, R. M., H. C. Jackson, R. M. May, and A. M. Smith. 1981. Population dynamics of fox rabies in Europe. Nature 289:765–771.
- Anderson, R. M., and R. M. May. 1991. Infectious diseases of humans. Oxford University Press, Oxford, UK.
- Biggs, J. R., K. D. Bennett, M. A. Mullen, T. K. Haarmann, M. Salisbury, R. J. Robinson, D. Keller, N. Torrez-Martinez, and B. Hjelle. 2000. Relationship of ecological variables to Sin Nombre virus antibody seroprevalence in populations of deer mice. Journal of Mammalogy 81:676–682.
- Bolker, B. M. 2008. Ecological models and data in R. Princeton University Press, Princeton, New Jersey, USA.
- Boone, J. D., E. W. Otteson, K. C. McGwire, P. Villard, J. E. Rowe, and S. C. St Jeor. 1998. Ecology and demographics of hantavirus infections in rodent populations in the Walker River basin of Nevada and California. American Journal of Tropical Medicine and Hygiene 59:445–451.
- Botten, J., K. Mirowsky, C. Ye, K. Gottlieb, M. Saavedra, L. Ponce, and B. Hjelle. 2002. Shedding and intracage transmission of Sin Nombre hantavirus in the deer mouse

- (Peromyscus maniculatus) model. Journal of Virology 76: 7587–7594.
- Calisher, C. H., J. J. Root, J. N. Mills, J. E. Rowe, S. A. Reeder, E. S. Jentes, K. Wagoner, and B. J. Beaty. 2005. Epizootiology of Sin Nombre and El Moro Canyon hantaviruses, southeastern Colorado, 1995–2000. Journal of Wildlife Diseases 41:1–11.
- Calisher, C. H., W. Sweeney, J. N. Mills, and B. J. Beaty. 1999. Natural history of Sin Nombre virus in western Colorado. Emerging Infectious Diseases 5:126–134.
- Carver, S., J. Trueax, R. Douglass, and A. Kuenzi. 2011. Delayed density-dependent prevalence of Sin Nombre virus infection in deer mice (*Peromyscus maniculatus*) in central and western Montana. Journal of Wildlife Diseases 47:56–63.
- Center for Disease Control. 1993. Outbreak of acute illness—southwestern United States, 1993. Morbidity and Mortality Weekly Report 42:421–424.
- Davis, S., E. Calvet, and H. Leirs. 2005. Fluctuating rodent populations and risk to humans from rodent-borne zoonoses. Vector-Borne and Zoonotic Diseases 5:305–314.
- Douglass, R. J., C. H. Calisher, K. D. Wagoner, and J. N. Mills. 2007. Sin Nombre virus infection of deer mice in Montana: characteristics of newly infected mice, incidence, and temporal pattern of infection. Journal of Wildlife Diseases 43:12–22.
- Douglass, R. J., T. Wilson, W. J. Semmens, S. N. Zanto, C. W. Bond, R. C. Van Horn, and J. N. Mills. 2001. Longitudinal studies of Sin Nombre virus in deer mouse-dominated ecosystems of Montana. American Journal of Tropical Medicine and Hygiene 65:33–41.
- Fairbairn, D. J. 1977. The spring decline in deer mice: death or dispersal? Canadian Journal of Zoology 55:84–92.
- Gao, L. Q., and H. W. Hethcote. 1992. Disease transmission models with density-dependent demographics. Journal of Mathematical Biology 30:717–731.

19399/10, 2015, 6, Downloaded from https://esajournals.on/heibtrary.wikey.com/doi/10.1890/14-1910.1 by Cochanne Uruguay, Wiley Online Library on [20/10.025]. See the Terms and Conditions (https://onlinebbrary.wiley.com/rems-and-conditions) on Wiley Online Library or rules of use; OA articles are governed by the applicable Creative Commons License

- Gill, J., and G. King. 2004. What to do when your Hessian is not invertible. Sociological Methods and Research 33:54–87.
- Glass, G. E., et al. 2000. Using remotely sensed data to identify areas at risk for hantavirus pulmonary syndrome. Emerging Infectious Diseases 6:238–247.
- Glass, G. E., J. E. Childs, G. W. Korch, and J. W. LeDuc. 1988. Association of intraspecific wounding with hantaviral infection in wild rats (*Rattus norvegicus*). Epidemiology and Infection 101:459–472.
- Glass, G. E., T. Shields, B. Cai, T. L. Yates, and R. Parmenter. 2007. Persistently highest risk areas for hantavirus pulmonary syndrome: potential sites for refugia. Ecological Applications 17:129–139.
- Glass, G. E., et al. 2002. Satellite imagery characterizes local animal reservoir populations of Sin Nombre virus in the southwestern United States. Proceedings of the National Academy of Sciences USA 99:16817–16822.
- Grenfell, B. T., and J. Harwood. 1997. (Meta)population dynamics of infectious diseases. Trends in Ecology and Evolution 12:395–399.
- Jones, C. G., R. S. Ostfeld, M. P. Richard, E. M. Schauber, and J. O. Wolff. 1998. Chain reactions linking acorns to gypsy moth outbreaks and Lyme disease risk. Science 279:1023–1026.
- Kausrud, K. L., H. Viljugrein, A. Frigessi, M. Begon, S. Davis, H. Leirs, V. Dubyanskiy, and N. C. Stenseth. 2007. Climatically driven synchrony of gerbil populations allows large-scale plague outbreaks. Proceedings of the Royal Society B 274:1963–1969.
- Kuenzi, A. J., R. J. Douglass, C. W. Bond, C. H. Calisher, and J. N. Mills. 2005. Long-term dynamics of Sin Nombre viral RNA and antibody in deer mice in Montana. Journal of Wildlife Diseases 41:473–481.
- Kuenzi, A. J., R. J. Douglass, D. White, Jr., C. W. Bond, and J. N. Mills. 2001. Antibody to Sin Nombre virus in rodents

- associated with peridomestic habitats in west central Montana. American Journal of Tropical Medicine and Hygiene 64:137–146.
- Linthicum, K. J., A. Anyamba, C. J. Tucker, P. W. Kelley, M. F. Myers, and C. J. Peters. 1999. Climate and satellite indicators to forecast rift valley fever epidemics in Kenya. Science 285:397–400.
- Luis, A. D., R. J. Douglass, J. N. Mills, and O. N. Bjørnstad. 2010. The effect of seasonality, density and climate on the population dynamics of Montana deer mice, important reservoir hosts for Sin Nombre hantavirus. Journal of Animal Ecology 79:462–470.
- Luis, A. D., R. J. Douglass, J. N. Mills, P. J. Hudson, and O. N. Bjørnstad. 2012. Sin Nombre hantavirus decreases survival of male deer mice. Oecologia 169:431–439.
- Madhav, N. K., K. D. Wagoner, R. J. Douglass, and J. N. Mills. 2007. Delayed density-dependent prevalence of Sin Nombre virus in Montana deer mice (*Peromyscus maniculatus*) and implications for human disease risk. Vector-Borne and Zoonotic Diseases 7:353–364.
- McCallum, H., N. Barlow, and J. Hone. 2001. How should pathogen transmission be modelled? Trends in Ecology and Evolution 16:295–300.
- McCallum, H., M. Jones, C. Hawkins, R. Hamede, S. Lachish, D. Sinn, N. Beeton, and B. Lazenby. 2009. Transmission dynamics of Tasmanian devil facial tumor disease may lead to disease-induced extinction. Ecology 90:3379–3392.
- Millar, J. S. 1989. Reproduction and development. Pages 169–232 in G. L. J. Kirkland and J. N. Layne, editors. Advances in the study of *Peromyscus* (Rodentia). Texas Tech University Press, Lubbock, Texas, USA.
- Mills, J. N., et al. 1997. Patterns of association with host and habitat: antibody reactive with Sin Nombre virus in small mammals in the major biotic communities of the southwestern United States. American Journal of Tropical Medicine and Hygiene 56:273–284.
- Mills, J. N., T. G. Ksiazek, C. J. Peters, and J. E. Childs. 1999a. Long-term studies of hantavirus reservoir populations in the southwestern United States: a synthesis. Emerging Infectious Diseases 5:135–142.

- Mills, J. N., T. L. Yates, T. G. Ksiazek, C. J. Peters, and J. E. Childs. 1999b. Long-term studies of hantavirus reservoir populations in the southwestern United States: rationale, potential, and methods. Emerging Infectious Diseases 5:95–101.
- Ostfeld, R. S., and F. Keesing. 2000. Pulsed resources and community dynamics of consumers in terrestrial ecosystems. Trends in Ecology and Evolution 15:232–237.
- Parmenter, R. R., J. W. Brunt, D. I. Moore, and S. Ernest. 1993. The hantavirus epidemic in the Southwest: rodent population dynamics and the implications for transmission of hantavirus-associated adult respiratory distress syndrome (HARDS) in the Four Corners region. Pages 1–45 in Report to the Federal Centers for Disease Control and Prevention. Sevilleta Long-Term Ecological Research Program, Department of Biology, University of New Mexico, Albuquerque, New Mexico, USA.
- R Development Core Team. 2010. R: a language and environment for statistical computing. R Foundation for Statistical Computing, Vienna, Austria. www.r-project.org
- Ramsey, D., N. Spencer, P. Caley, M. Efford, K. Hansen, M. Lam, and D. Cooper. 2002. The effects of reducing population density on contact rates between brushtail possums: implications for transmission of bovine tuberculosis. Journal of Applied Ecology 39:806–818.
- Saitoh, T., and K. Takahashi. 1998. The role of vole populations in prevalence of the parasite (*Echinococcus multilocularis*) in foxes. Researches on Population Ecology 40:97–105.
- Smith, M. J., S. Telfer, E. R. Kallio, S. Burthe, A. R. Cook, X. Lambin, and M. Begon. 2009. Host-pathogen time series data in wildlife support a transmission function between density and frequency dependence. Proceedings of the National Academy of Sciences USA 106:7905–7909.
- Venables, W. N., and B. D. Ripley. 2002. Modern applied statistics with S. Springer, New York, New York, USA.
- Wood, S. N. 2001. Partially specified ecological models. Ecological Monographs 71:1–25.
- Yates, T., J. N. Mills, C. A. Parmenter, and T. G. Ksiazek. 2002. The ecology and evolutionary history of an emergent disease: hantavirus pulmonary syndrome. BioScience 52:989–

SUPPLEMENTAL MATERIAL

**Ecological Archives** 

The Appendix is available online: http://dx.doi.org/10.1890/14-1910.1.sm